

Bayesian shared parameter joint models for heterogeneous populations

Sida Chen*, Danilo Alvares, Marco Palma, Jessica K. Barrett

MRC Biostatistics Unit, University of Cambridge, U.K.

**email*: sida.chen@mrc-bsu.cam.ac.uk

Abstract

Joint models (JMs) for longitudinal and time-to-event data are an important class of biostatistical models in health and medical research. When the study population consists of heterogeneous subgroups, the standard JM may be inadequate and lead to misleading results. Joint latent class models (JLCMs) and their variants have been proposed to incorporate latent class structures into JMs. JLCMs are useful for identifying latent subgroup structures, obtaining a more nuanced understanding of the relationships between longitudinal outcomes, and improving prediction performance. We consider the generic form of JLCM, which poses significant computational challenges for both frequentist and Bayesian approaches due to the numerical intractability and multimodality of the associated model's likelihood or posterior. Focusing on the less explored Bayesian paradigm, we propose a new Bayesian inference framework to tackle key limitations in the existing method. Our algorithm leverages state-of-the-art Markov chain Monte Carlo techniques and parallel computing for parameter estimation and model selection. Through a simulation study, we demonstrate the feasibility and superiority of our proposed method over the existing approach. Our simulations also generate important computational insights and practical guidance for implementing such complex models. We illustrate our method using data from the PAQUID prospective cohort study, where we jointly investigate the association between a repeatedly measured cognitive score and the risk of dementia and the latent class structure defined from the longitudinal outcomes.

Keywords: Bayesian inference; Clustering; Joint model; Longitudinal data; Mixture model.

1 Introduction

In many clinical and epidemiological studies, repeated measurements of biological markers and time-to-event data are simultaneously collected. For instance, in cohort studies on chronic conditions such as cardiovascular disease and lung disease, there has been great interest in characterizing the association patterns between marker trajectories and key health events, such as disease progression or death (Barrett et al. 2019, Su

et al. 2021). Joint models (JMs) have become an increasingly popular statistical modelling framework for jointly analyzing such longitudinal and time-to-event outcomes and demonstrate great potential for advancing medical insights and supporting patient monitoring (Rizopoulos 2012, Papageorgiou et al. 2019).

In some scenarios, such as multi-center studies, the study population may naturally consist of heterogeneous sub-populations, with each one exhibiting potentially different longitudinal and time-to-event profiles. It may also be the case that there is additional heterogeneity that cannot be well explained by the recorded variables. In these situations, the standard JM may no longer be appropriate, and a naive implementation could lead to misleading inference results and conclusions. Joint latent class models (JLCMs) arise as an alternative framework to the standard JM, which explicitly model the latent subgroup structure by adopting a mixture model approach (see Proust-Lima et al. (2014) for an overview). A fundamental assumption underlying the basic JLCM is the conditional independence of the longitudinal and time-to-event outcomes given the latent class membership, in other words, that implies that the association between the two outcome processes are fully explained via the shared latent class. While this assumption greatly alleviates the computational burden in model estimation, it no longer offers straightforward interpretation on the association structure between the longitudinal and time-to-event outcomes, which would be of interest in many clinical studies. Additionally, violation of this assumption could potentially necessitate the use of a larger number of latent classes, making them less interpretable. Therefore, the basic JLCM is mostly useful for prediction problems.

To improve modelling flexibility and interpretability, the basic JLCM has been extended in more recent works in order to introduce additional dependency between the outcomes within each class. This is achieved by sharing random effects across the longitudinal and time-to-event submodels, and we refer to the resulting models as shared parameter JLCMs (see, e.g., Liu et al. (2015, 2020), Andrinopoulou et al. (2020), Wong et al. (2022)). These models, however, introduce new challenges to statistical inference due to the presence of high-dimensional discrete and continuous latent variables. In frequentist methods, estimation is performed by maximizing the marginal likelihood function with all latent variables integrated out. For shared parameter JLCMs, this can be computationally prohibitive due to the need for numerical approximations to handle the integrals over random effects, and optimization can be challenging due to the presence of multiple local maxima. For Bayesian methods, inference is based on the posterior distribution of model parameters, along with the latent variables, and numerical integration with respect to random effects is not required. Available information on the data can be incorporated via priors, which can also have a regularizing effect on inference. In this paper, we focus on the Bayesian paradigm due to its appeal from both modelling and computational perspectives. To our knowledge, the only existing Bayesian method is that proposed by Andrinopoulou et al. (2020), who introduced a two-stage estimation framework. In stage 1, an overfitted mixture (a mixture with potentially more classes than necessary) is employed to infer the number of latent classes by removing ‘empty’ classes. In stage 2, conditional on the results from stage 1, a shared parameter JLCM is refitted. However, there are several limitations to this approach. One challenge with the overfitted mixture model is that it can be computationally difficult to fit due to its complexity. Additionally, the number of latent classes inferred is highly sensitive to a threshold parameter, which requires tuning. Andrinopoulou et al. (2020) used classical

Markov chain Monte Carlo (MCMC) methods, implemented in JAGS, for posterior sampling. However, with high-dimensional and multimodal posterior spaces, such as in this model, these MCMC methods may suffer from poor mixing and convergence issues. Another important issue not properly addressed in their work is the presence of multimodality in the posterior, even with label ordering constraints. This issue can be particularly significant when using standard noninformative priors, as is commonly done in JMs. In such scenarios, relying on a single MCMC chain can lead to biased inference.

In this paper, we propose a new Bayesian inference framework for shared parameter JLCMs, addressing some of the key limitations of existing Bayesian approaches. Our method is built on a finite mixture model framework. We consider models with plausible numbers of latent classes. A more appropriate model for the given data can then be selected through Bayesian model comparison, which may be conducted using suitable information criteria. From the modelling perspective, we found that using mildly informative priors can be highly advantageous for shared parameter JLCMs, as they help with model identifiability and improve MCMC convergence. These priors can be informed by available domain knowledge or through an empirical Bayes approach. To perform posterior inference for a given model, differently from Andrinopoulou et al. (2020), we utilize the No-U-Turn Sampler (NUTS), an auto-tuned Hamiltonian Monte Carlo algorithm, for sampling all continuous parameters (Hoffman et al. 2014). NUTS is particularly advantageous when the posterior is of high dimensionality and complexity, and is widely regarded as the state-of-the-art MCMC method (Štrumbelj et al. 2024). To appropriately handle the multimodal posterior, we propose a computationally simple yet effective approach that involves embarrassingly parallel MCMC sampling, leveraging multi-core computing. The effectiveness of our proposed method, and its superiority over the existing approach, is demonstrated through a simulation study that follows and extends the settings considered in Andrinopoulou et al. (2020). We further illustrate the method using data from the well-known PAQUID prospective cohort study (Letenneur et al. 1994), accessed via the `1cmm` R package (Proust-Lima et al. 2023). In this analysis, we investigate the latent subgroup structure within the population and examine the relationship between cognitive aging and the risk of dementia.

The rest of this paper is structured as follows. In Section 2, we present the formulation of the shared parameter JLCM. Section 3 discusses several key aspects related to the Bayesian estimation of the joint model. In Section 4, we present a simulation study to compare our method with the existing approach and investigate the impact of a specific model misspecification. An application to data from the PAQUID cohort study is presented in Section 5. Finally, Section 6 concludes with a discussion of the proposed method and potential future perspectives.

2 Shared parameter joint latent class models

In this section we present the model in its general form. We assume the population of sample size n consists of a fixed G latent classes, where G may be unknown. Each latent class is characterized by a class-specific joint distribution of the longitudinal and time-to-event outcomes formed via shared random effects. The model consists of the following three submodel components.

2.1 The class membership submodel

Let c_i denote the latent class membership indicator for individual i , $i = 1, \dots, n$, with $c_i = g$, $g = 1, \dots, G$, if subject i belongs to the g th class. The indicator c_i is unobserved and is modelled using a categorical distribution with a probability vector $\pi_i = (\pi_{i1}, \dots, \pi_{iG})$, where $\pi_{ig} = P(c_i = g)$. The membership probabilities are typically related to a set of p -dimensional time-independent baseline covariates W_i , via the softmax link function

$$\pi_{ig} = P(c_i = g | W_i) = \frac{\exp(\psi_{g0} + W_i^T \psi_g)}{\sum_{k=1}^G \exp(\psi_{k0} + W_i^T \psi_k)}, \quad g = 1, \dots, G, \quad (1)$$

where $\psi_g = (\psi_{g1}, \dots, \psi_{gp})$ are the class-specific vectors of regression coefficients associated with W_i . For identifiability purpose, we set ψ_{G0} and ψ_G to zeros. When no external covariates are considered, the membership probability vector becomes the same across all subjects, i.e., $\pi_i = \pi$ for all i . In this scenario, Andrinopoulou et al. (2020) proposed an alternative model, where π is directly modelled on the simplex using a Dirichlet distribution. However, with this approach, incorporating covariates is difficult, and as we will show in Section 4, the omission of relevant covariates can be problematic as it can introduce estimation bias to other model parameters.

2.2 The longitudinal submodel

Let $y_i(t)$ denote the value of the longitudinal outcome of subject i measured at time t , and let $y_i = (y_{i1}, \dots, y_{in_i})$ be the observed n_i -dimensional longitudinal response vector, where $y_{ij} = y_i(t_{ij})$, $j = 1, \dots, n_i$. Conditional on the latent class g , the longitudinal outcome is typically modelled using a generalized linear mixed model (GLMM) framework. An important difference from the standard JM ($G = 1$) is that we now need to introduce class-specific random effects b_{ig} to characterize the deviation of a subject's marker trajectory relative to the average marker trajectory of class g . Assuming the same set of random effects across classes (i.e., $b_{i1} = b_{i2} = \dots = b_{iG}$) can, therefore, be problematic and may lead to biased inference. Denote $b_i = (b_{i1}, b_{i2}, \dots, b_{iG})$. Assuming that the r -dimensional random effect vector b_{ig} is distributed according to a multivariate normal distribution $N(0, \Sigma_g)$, then given $c_i = g$ and b_i , the response y_{ij} are assumed to be independent and belong to a member of the exponential family with density

$$f(y_{ij} | c_i = g, b_i) = \exp \left\{ \frac{y_{ij} \zeta_{ij}(b_{ig}) - a_1(\zeta_{ij}(b_{ig}))}{a_2(\eta_g)} - a_3(y_{ij}; \eta_g) \right\}, \quad (2)$$

where $\zeta_{ij}(b_{ig})$ and η_g denote the natural and dispersion parameters in the exponential family, respectively, and $a_1(\cdot)$, $a_2(\cdot)$, and $a_3(\cdot)$ are known functions specifying the member of the exponential family. The conditional mean of y_{ij} given the class membership and random effects is related to the linear predictors via

$$E[y_{ij} | c_i = g, b_i, X_i(t), Z_i(t)] = a'_1(\zeta_{ij}) = g^{-1}(X_i^T(t_{ij})\beta_g + Z_i^T(t_{ij})b_{ig}), \quad (3)$$

where $a'_1(\cdot)$ denotes the first derivative with respect to its argument, $g(\cdot)$ denotes a known monotonic link function specified according to the member of the exponential family, β_g is a vector of class-specific regression

coefficients, and $X_i^T(t)$ and $Z_i^T(t)$ denote the possibly time-dependent design vectors for the fixed and random effects, respectively. In the case of continuous longitudinal response, the GLMM reduces to a standard Gaussian linear mixed model (LMM):

$$(y_{ij} | c_i = g, b_i) \sim N(\mu_i(t_{ij} | c_i = g, b_i, X_i(t), Z_i(t)), \sigma_g^2), \quad (4)$$

where $\mu_i(t_{ij} | c_i = g, b_i, X_i(t), Z_i(t)) = X_i^T(t_{ij})\beta_g + Z_i^T(t_{ij})b_{ig}$ and σ_g^2 is the class-specific error variance.

2.3 The time-to-event submodel

Let T_i^* be the true event time of interest and C_i be the censoring time for subject i . We define the observed event time as $T_i = \min(T_i^*, C_i)$, and the censoring indicator variable $\Delta_i = I(T_i^* \leq C_i)$, where $I(\cdot)$ is the indicator function. Conditional on the latent class membership, we model the risk of the event via the class-specific hazard function as

$$h_i(t | c_i = g, b_i, \tilde{W}_i) = h_{0g}(t) \exp \left\{ \tilde{W}_i^T \gamma_g + f(\beta_g, b_{ig}, t, \alpha_g) \right\}, \quad (5)$$

where $h_{0g}(t)$ is the baseline hazard function parameterized by ϕ_g , γ_g denotes the vector of regression coefficients associated with the vector of exogenous risk factors \tilde{W}_i , and $f(\cdot)$ serves the role to link the longitudinal and the time-to-event processes within a latent class. In this paper, we consider the so-called current value association structure, where $f(\cdot) = \alpha_g \mu_i(t_{ij} | c_i = g, b_i, X_i, Z_i)$, with α_g characterizing the strength of the association. This is perhaps the most popular option in the JM literature but other reasonable functional forms may be considered, depending on the application context. Note that without the inclusion of the function $f(\cdot)$, (5) reduces to a standard proportional hazard model and the resulting full model becomes the basic JLCM of Proust-Lima et al. (2014).

3 Bayesian inference

3.1 The Bayesian model

Let the full dataset $D^{(n)} = (D_1, \dots, D_n)$, where $D_i = (y_i, T_i, \Delta_i)$, $c = (c_1, \dots, c_n)$, $\mathbf{b} = (b_1, \dots, b_n)$, and let $\Theta = (\{\psi_{g0}\}_{g=1}^{G-1}, \{\psi_g\}_{g=1}^{G-1}, \{\eta_g\}_{g=1}^G, \{\beta_g\}_{g=1}^G, \{\phi_g\}_{g=1}^G, \{\alpha_g\}_{g=1}^G, \{\gamma_g\}_{g=1}^G, \{\Sigma_g\}_{g=1}^G)$ denote the collection of all parameters associated with the model presented in Section 2. We assume that the joint posterior density of model parameters, random effects and latent class indicator variables, takes the form

$$\begin{aligned} p(\Theta, \mathbf{b}, \mathbf{c} | D^{(n)}) &\propto \prod_{i=1}^n \left(p(D_i | b_i, c_i, \Theta) p(c_i | \Theta) \prod_{g=1}^G p(b_{ig} | \Theta) \right) \times p(\Theta) \\ &= \prod_{i=1}^n \left(\prod_{g=1}^G (p(y_i | b_i, c_i = g, \Theta) p(T_i, \Delta_i | b_i, c_i = g, \Theta) \pi_{ig})^{I(c_i=g)} p(b_{ig} | \Theta) \right) \times p(\Theta), \end{aligned} \quad (6)$$

where $p(y_i | b_i, c_i = g, \Theta)$ is given by (2) and (3), π_{ig} is given by (1), and $p(b_{ig} | \Theta)$ is the density of multivariate normal distribution with mean 0 and covariance matrix Σ_g . $p(T_i, \Delta_i | b_i, c_i = g, \Theta)$ is the likelihood contribution from the survival submodel, which takes the form

$$p(T_i, \Delta_i | b_i, c_i = g, \Theta) = h_i(t | c_i = g, b_i)^{I(\Delta_i=1)} \times \exp \left\{ - \int_0^{T_i} h_i(s | c_i = g, b_i) ds \right\}, \quad (7)$$

where the hazard function h_i is given by (5). The integral in (7) cannot be computed analytically in general and numerical approximation is required. In our implementation, we used the Gaussian-Legendre quadrature method (with 15 quadrature points).

We assume that the joint prior density $p(\Theta)$ is factorized into a product of prior density for each parameter. For the model in consideration, prior specification requires some care. Either overly strong or vague priors could be problematic: the former prior setting could have strong and undesirable influence on inference, such as on the selection of number of latent classes (see Section 3.4), especially when the sample size is small, whereas the latter setting may lead to a highly multi-modal posterior and MCMC could show mixing issues. To help with model identifiability and MCMC sampling efficiency, we propose to use mildly informative priors where possible. Hyperparameters can be selected based on available information for the data and expected structure for the resulting model, and/or guided by an empirical Bayes approach.

We want to give special attention to the priors for the variance parameters given their important contribution to the posterior and the specific structure of the mixture model. Standard default noninformative choices, such as the inverse gamma prior with extremely small shape and scale parameters, may not be appropriate when $G > 1$. When the LMM is used for the longitudinal submodel, we can use the popular half-Normal distribution as a prior on the residual error variance σ_g^2 . Since σ_g^2 is not expected to be influenced much by the time-to-event data or varying values of G , the hyperparameter can be selected based on a LMM fit (with $G = 1$) to the longitudinal data alone. Light-tailedness of the normal distribution is desirable to prevent excessively large values. In this paper, we assume the covariance matrices Σ_g to be diagonal, so setting the prior for Σ_g amounts to setting the prior for the random effect variances. Note that the random effects are still allowed to be correlated *a posteriori* if supported by the data, as there is no independence constraint in the posterior distribution of the random effects. Heuristically, we want the prior to prevent both excessively small and large values. Extremely small random effect variances may be associated with the formation of ‘small’ clusters or cluster degeneracy, and mixing issues can occur when the variance approaches zero due to instability in the posterior. In contrast, large values could conflict with the latent classes’ role in explaining population heterogeneity, coincide with the formation of a ‘large’ class, and/or the collapse of other classes. In our implementation, we have found that a Gamma distribution with equal shape and rate parameters greater than 1 provides a good choice to cover variance values within a reasonable range. To get an idea of the plausible range of random effects variances for a specific model, we can fit a basic JLCM conditional on different candidate values of G using the MLE approach developed in Proust-Lima et al. (2017), implemented via the `lcmm` R package, noting that random effects variances are generally expected to decrease as G increases. Later, in Sections 4 and 5, we provide concrete examples and explanations regarding

the choice of priors.

3.2 Posterior sampling

The resulting posterior distribution defined via equation (6) is not analytically tractable so we resort to MCMC methods for posterior inference. We consider the NUTS algorithm due to its efficiency for sampling from high dimensional parameter spaces. NUTS requires the underlying density to be smooth because it relies on gradient computation, so it cannot be used to directly sample from (6) due to the presence of discrete variables. Instead, we use NUTS to sample from the posterior with c_i marginalized out from (6), $p(\Theta, b | D^{(n)})$, which is proportional to

$$\prod_{i=1}^n \left[\left(\sum_{g=1}^G p(y_i | b_i, c_i = g, \Theta) p(T_i, \Delta_i | b_i, c_i = g, \Theta) \pi_{ig} \right) \prod_{g=1}^G p(b_{ig} | \Theta) \right] \times p(\Theta). \quad (8)$$

Posterior samples of latent class allocation variable c_i can be obtained by sampling exactly from its full conditional distribution $p(c_i | \Theta^{(j)}, b^{(j)}, D^{(n)})$, which is a categorical distribution with weights for class g , $g = 1, \dots, G$, proportional to

$$p(y_i | b_i^{(j)}, c_i = g, \Theta^{(j)}) p(T_i, \Delta_i | b_i^{(j)}, c_i = g, \Theta^{(j)}) \pi_{ig}^{(j)}, \quad (9)$$

where $b_i^{(j)}$ and $\Theta^{(j)}$ are the j th MCMC samples from $p(\Theta, b | D^{(n)})$, and $\pi_{ig}^{(j)}$ is computed using $\Theta^{(j)}$. Note that based on the sampled c_i , the posterior class membership probability can be estimated as

$$\hat{p}(c_i = g | D^{(n)}) = \frac{1}{T} \sum_{j=1}^T I(c_i^{(j)} = g), \quad i = 1, \dots, n, \quad g = 1, \dots, G. \quad (10)$$

3.3 Tackling multimodality in the posterior

For mixture-type models, an obvious cause of multimodality in the posterior is the invariance of the likelihood under permutations of the latent class labels. This can create problems for MCMC-based inference because label switching may occur (in theory) during MCMC runs, rendering the marginal posterior for class-specific parameters unidentifiable. To ensure valid inference, some kind of post-processing of MCMC samples is required, see, e.g., Stephens (2000). However, in complex hierarchical models like the one considered here, label switching is nearly impossible within a practical number of MCMC runs because it requires a simultaneous jump for all class-specific parameters. In our experiments, label switching did not occur for our models.

What needs to be tackled is that multiple well-separated local regions of high density can still appear in the posterior, even within the space of a specific class labelling. This is observed in MCMC runs (especially with the use of noninformative priors) and is overlooked in Andrinopoulou et al. (2020). This makes single-chain MCMC inference problematic, as the chain may get trapped in a local region depending on the location of initialization. Various MCMC schemes have been proposed in the literature to handle complex multimodal distributions, notably parallel tempering, which involves running multiple chains that communicate with

each other. However, effective use of such algorithms requires careful design and tuning, and they can be computationally prohibitive for complex models. Our idea here is motivated by (Yao et al. 2022), who propose a Bayesian stacking approach to take advantage of fully parallel MCMC sampling, aiming to combine locally stuck chains to enhance prediction performance. When the focus is on inference, a modification leads to a sampling scheme with the following three steps:

1. Run M parallel chains with different initializations.
2. Clustering the M parallel chains into K clusters, defined over regions $\Omega_1, \dots, \Omega_K$, with $K \leq M$.
3. Select a region Ω_k with probability proportional to

$$w_k = \int P(D | b, \Theta) P(b | \Theta) P(\Theta) \mathbb{I}((b, \Theta) \in \Omega_k) db d\Theta,$$

and then draw a sample with replacement from Ω_k .

In step 2, a between-chain mixing measure such as \hat{R} can be used for clustering the chains (Vehtari et al. 2021), and the weights w_k can be estimated by any valid Monte Carlo estimator for the marginal likelihood based on samples in Ω_k (Llorente et al. 2023). Assuming that the chains cover all important regions of the support, the final samples would form approximate samples from the target posterior, as this is essentially a importance resampling procedure (Smith & Gelfand 1992).

When the dimensionality of the parameter space becomes high, the clustering procedure in step 2 can still be challenging to implement. To improve computational feasibility, in our implementation, we consider a simplified version of the scheme above with the clustering step removed, and we select one among the M parallel chains that produces the highest weights, upon which inference will be based. This approach can be justified with the assumption that the posterior is dominated by a single region Ω_k^* in terms of posterior mass, which may be reasonable with the use of mildly informative priors, or, if we are willing to use the model that provides the largest probability given the data. In our simulations, we found this simplified scheme performed satisfactorily. Note that the posterior within Ω_k may still have a complex structure; therefore, it remains important that the MCMC algorithm is efficient so that it adequately explores the local region, which motivates our choice of the NUTS algorithm. In our implementation, to estimate the weights w_k , we consider the truncated harmonic mean estimator (Robert & Wraith 2009, Chen & Finkenstädt 2023), which is given by

$$\left(\frac{1}{T} \sum_{i=1}^T \frac{h(b^{(i)}, \Theta^{(i)})}{p(D^{(n)} | b^{(i)}, \Theta^{(i)}) p(b^{(i)}, \Theta^{(i)})} \right)^{-1}, \quad (11)$$

where $b^{(i)}$ and $\Theta^{(i)}$ are the i th MCMC samples out of a total of T samples. A convenient choice for h is

$$h(b, \Theta) = \frac{1}{V(\epsilon)\beta T} \sum_{j: (b^{(j)}, \Theta^{(j)}) \in \mathcal{H}_\beta} \mathbb{I}(d((b^{(j)}, \Theta^{(j)}), (b, \Theta)) < \epsilon), \quad (12)$$

where $V(\epsilon)$ is the volume of the ball centered at (b, Θ) with radius ϵ (small), $\mathcal{H}_\beta = \{(b^{(j)}, \Theta^{(j)}) : p(D^{(n)} | b^{(j)}, \Theta^{(j)}) p(b^{(j)}, \Theta^{(j)}) > q_\beta\}$, and q_β is the empirical upper β quantile of $p(D^{(n)} | b^{(i)}, \Theta^{(i)}) p(b^{(i)}, \Theta^{(i)})$.

When the radius is sufficiently small, $h(\mathbf{b}^{(i)}, \Theta^{(i)})$ will take the value of $1/(V(\epsilon)\beta T)$ if the sample is from \mathcal{H}_β , and zero otherwise. Note also that $V(\epsilon)$ does not need to be computed, as it will cancel out during normalization. To further aid in convergence, we initialize the chains making use of the MLE obtained under the basic JLCM via the `lcmm` R package. More specifically, initial values for $\eta_g, \beta_g, \phi_g, \gamma_g$ are motivated by the MLE, followed by a random perturbation. All other parameters and latent variables are randomly initialized.

3.4 Selection of number of classes

In many application contexts, the number of latent classes G , if any, is unknown. To infer this value, we choose not to adopt the overfitted mixture approach proposed by Andrinopoulou et al. (2020) due to the aforementioned difficulties. Instead, we propose simultaneously considering models with candidate values of G , treating it as a model comparison problem. One popular class of methods for Bayesian model choice is based on marginal likelihood or Bayes factors, which generally have consistency in model selection when the true generating process is among the candidate models, though it is worth noting that, in practice, seeking the ‘true’ number of classes may not be meaningful or realistic. An important issue with these approaches is that the results can be sensitive to the choice of priors. For our model, we find that the prior for the random effect variances can have a strong influence on the estimated marginal likelihood.

Here, we consider a different class of methods to guide our choice on G , which are based on expected predictive error or generalization loss. The two most popular criteria for this purpose are the Bayesian leave-one-out information criterion (LOOIC) and the widely applicable information criterion (WAIC) (Vehtari et al. 2017). LOOIC targets $\sum_{i=1}^n \log p(D_i | D_{-i})$ (or multiplied by -2 to be on the deviance scale), where in our context $p(D_i | D_{-i}) = \int p(D_i | \mathbf{b}, \mathbf{c}, \Theta) p(\mathbf{b}, \mathbf{c}, \Theta | D_{-i}) d\mathbf{b} d\mathbf{c} d\Theta$. WAIC, on the other hand, targets $\sum_{i=1}^n \log p(D_i | D^{(n)}) - p_{\text{WAIC}}$ (or multiplied by -2 to be on the deviance scale), where $p(D_i | D^{(n)}) = \int p(D_i | \mathbf{b}, \mathbf{c}, \Theta) p(\mathbf{b}, \mathbf{c}, \Theta | D^{(n)}) d\mathbf{b} d\mathbf{c} d\Theta$, and p_{WAIC} is defined as the sum of the posterior variance of the log predictive density for each data point. To compare two models, we examine the significance of the difference in predictive performance by comparing the z-score, which is computed by dividing the estimated difference in LOOIC or WAIC by the estimated standard error associated with the difference, to the critical value for a one-tailed test based on the standard normal distribution at a given significance level (Sivula et al. 2020). The two criteria and the quantities required for computing the z-score can be estimated based on MCMC outputs using the method developed in Vehtari et al. (2017), which is implemented in the `loo` R package (Vehtari et al. 2024). In line with the parsimony principle, a more complex model should be selected only if it demonstrates a statistically significant improvement. In our experience (see also results in Section 4), we found that a relatively stringent significance level, such as $\alpha = 0.1\%$, is necessary to guard against the risk of overfitting. We want to emphasize that in practice, one should not blindly follow results based on such criteria, as they can be influenced by deviations in model formulation from the unknown true data-generating process (if one exists) and the quality of the estimates of these criteria. Therefore, these results should be considered with cautiousness in conjunction with model interpretation and the application context.

4 Simulation study

We consider a simulation study consisting of two simulation settings. Setting I follows exactly from the simulation study considered in Andrinopoulou et al. (2020), with the aim of providing a ‘sanity check’ for the proposed method and evaluating the performance of our approach in comparison to theirs. Setting II, modified from Setting I, aims to evaluate the impact of the misspecification of the class membership submodel on inference.

4.1 Simulation settings

4.1.1 Setting I

In this setting, three scenarios are considered for the latent class structure, with G equals one, two and three. The total sample size is fixed at $n = 900$, and the latent class membership is randomly assigned to each individual according to pre-specified proportions of each class. The class-specific longitudinal trajectory is generated from a LMM specified as

$$y_i(t) = \beta_{g0} + \beta_{g1}t + b_{ig0} + b_{ig1}t + \beta_{g2}\text{male}_i + \epsilon_{ig}(t), \quad (13)$$

where $\epsilon_{ig}(t) \sim N(0, \sigma_g^2)$, $(b_{ig0}, b_{ig1}) \sim N(0, \Sigma_g)$, and male_i is an artificial covariate for gender, simulated from a Bernoulli distribution with a probability 0.5 for being male (labelled as 1). The class-specific time-to-event model is specified as

$$h_i(t) = \phi_{g0}t^{\phi_{g0}-1} \exp\{\phi_{g1} + \gamma_{g1}\text{age}_i + \alpha_g\mu_i(t)\}, \quad (14)$$

where $\mu_i(t) = \beta_{g0} + \beta_{g1}t + b_{ig0} + b_{ig1}t + \beta_{g2}\text{male}_i$. age_i is generated from a normal distribution centered at 45 with a standard deviation of 15.70. For each individual, a random censoring time C_i is generated from a uniform distribution between zero and 17.5. We refer to Andrinopoulou et al. (2020) (Table 1) for further details on parameter value settings. For each scenario, we evaluated the performance of LOOIC and WAIC in selecting the number of classes by considering candidate values of G ranging from one to four, and we considered three significance levels ($\alpha = 5\%$, 1% , 0.1%) for performing the model comparison as described in Section 3.4. Conditional on the true value of G , we further examine the performance of the proposed algorithm in terms of accuracy in parameter estimation and classification. Under Setting I, the estimation model (for a given G) assumes the same model formulation for both the longitudinal and survival submodels as used in the generating process, with no covariates included in the membership submodel.

4.1.2 Setting II

For this setting we have fixed $G = 2$. The data generation process for the longitudinal and survival submodel are the same as in Setting I. We consider 4 different scenarios to generate the class membership:

- Scenario 1: class allocation independent of any covariates (same as Setting I with $G = 2$).
- Scenario 2: $W_i = \tilde{x}_i$, where $\tilde{x}_i \sim N(0, 1)$, with $\psi_{10} = -0.4$, $\psi_{11} = 1$.

- Scenario 3: $W_i = (\text{male}_i, \text{age}_i)$, with $\psi_{10} = 2$, $\psi_{11} = 4$, $\psi_{12} = -0.1$.
- Scenario 4: $W_i = (\text{male}_i, \text{age}_i, \tilde{x}_i)$, with $\psi_{10} = 2$, $\psi_{11} = 4$, $\psi_{12} = -0.1$, $\psi_{13} = 1$.

For each scenario, we consider two estimation models, which represent two common choices for modelling the class membership. Model 1 assumes homogeneous class membership probabilities as used in Setting I (i.e., correctly specified for Scenario 1), whereas model 2 considers the same set of covariates as considered in class-specific JM with $W_i = (\text{male}_i, \text{age}_i)$ (i.e., correctly specified for Scenario 3). Results from the two estimation models are compared in terms of the accuracy of estimating the commonly shared parameters, as well as classification accuracy.

4.2 Estimation settings

To implement the proposed algorithm, we use the following set of priors for the model parameters throughout:

$$\begin{aligned} \beta_{gi}, \gamma_{gi}, \phi_{g1}, \alpha_g &\sim N(0, 5^2), \quad \psi_{gi} \sim N(0, 2^2), \quad \phi_{g0} \sim \text{Gamma}(2, 0.5), \\ \sigma_g^2 &\sim \text{half-Normal}(0, 0.5^2), \quad \Sigma_{g,ii} \sim \text{Gamma}(1.5, 1.5), \end{aligned} \tag{15}$$

where $\text{Gamma}(\alpha, \beta)$ represents a Gamma distribution with shape parameter α and rate parameter β , $\text{half-Normal}(\mu, \sigma^2)$ denotes a half-Normal distribution with location parameter μ and scale parameter σ , and $\Sigma_{g,ii}$ denotes the i th diagonal entry of Σ_g . For fixed effect and association parameters (β_{gi} , γ_{gi} , ϕ_{g1} and α_g), the priors are weakly informative, similar to those used in standard JMs. We use a slightly more informative prior for the fixed effect parameters ψ_{gi} in the class membership submodel to prevent the resulting mixture weights from getting too close to the boundary of the simplex. For the Weibull shape parameter ϕ_{g0} , the Gamma prior we use has a flat, unimodal shape and right skewness, covering plausible values in survival analysis. For the variance parameters, the prior hyperparameters are partly informed from an empirical Bayes perspective. For σ_g^2 , the scale parameter in the half-Normal prior is chosen to be close to the MLE results obtained from fitting a LMM to the longitudinal data. The shape and rate parameters in the Gamma prior for $\Sigma_{g,ii}$ are chosen to be 1.5 (for $G > 1$), which is found to sufficiently cover plausible values of the random effects variance (for $G = 2, 3, 4$). When fitting the model with $G = 1$, i.e., no latent class, we use the same prior settings as in (15), except that for $\Sigma_{g,ii}$, we use an inverse gamma prior with shape and scale parameters set to 0.01, which is a common weakly informative choice for the standard JM.

To perform posterior sampling, as described in Section 3.2, we used the Stan modelling language via the R interface provided by the `rstan` R package (Stan Development Team 2024), which provides a convenient implementation of the NUTS. In our simulations, we used the default settings for the optional tuning parameters in NUTS, as they generally worked well and achieved a good balance between sampling and computational efficiency. However, in practice, for complex models where divergent transitions or stability issues arise, these default settings can be adjusted. For example, the target acceptance rate (referred to as `adapt_delta`) can be increased from the default value of 0.8 to a larger value (such as 0.9 or higher) to improve the robustness of NUTS, although higher values may substantially increase sampling time. To implement the parallel sampling

scheme as described in Section 3.3, we used $M = 6$ parallel chains, each run for 5500 iterations, with the first 2500 iterations discarded as burn-in. For each chain, the 3000 post-burn-in samples were further thinned by an interval of 3. These settings were found to be sufficient for our simulation; however, in more challenging scenarios, more chains, a longer burn-in period, or a larger thinning interval may be required. To estimate the weights for each chain using the truncated harmonic mean estimator, we used $\beta = 0.6$ (but the results seem generally robust for different values of this parameter). All computations were performed on the Cambridge Service for Data Driven Discovery (CSD3) High-Performance Computing (HPC) system using the Ice Lake CPUs.

4.3 Results

Table 1 summarizes the performance of LOOIC and WAIC in model selection under simulation Setting I, with results obtained using the procedure described in Section 3.4. LOOIC consistently outperforms WAIC, and as the significance level becomes more stringent, the performance of both criteria improves. When compared to the results reported in Andrinopoulou et al. (2020) (see Table 3 therein for details), which shows proportions of the true number of classes selected at 30%, 49% and 72% for scenarios 1, 2 and 3 respectively, conditional on the best-performed tuning parameter, both LOOIC (at all significance levels) and WAIC (at $\alpha = 0.1\%$) demonstrate superior accuracy across all three scenarios. Figures 1 and 2 in the supplementary material displays the results of LOOIC and WAIC (on the deviance scale, where lower values indicate better performance) across replications of the data. It is interesting to note that both criteria exhibit a general pattern where the estimates stabilise once the number of latent classes reaches the true value. It also becomes clear that there is a potential risk of overfitting if one simply selects the model with the lowest value. Supplemental Tables 1 and 2 (under Model 1) present the estimation results conditional on $G = 3$ and $G = 2$, respectively. Our proposed algorithm demonstrates satisfactory performance in both point and interval estimation. With regard to classification accuracy, defined as the proportion of correctly classified subjects based on the maximum *a posteriori* (MAP) decision rule, and with class allocation probabilities computed as described in Section 3.2, we achieve consistently high accuracy. The median and interquartile range summarized from 200 replications are 98.8% (98.6%, 99.0%) for $G = 2$ and 99.4% (99.2%, 99.6%) for $G = 3$, respectively.

For simulation Setting II, Tables 2 and 3 summarise the estimation results for Scenarios 3 and 4, respectively, while results for Scenarios 1 and 2 are presented in Supplemental Tables 2 and 3. Model 1, which ignores covariates in class membership submodel, can incur significant bias and much lower coverage for certain parameters when the true class allocation depends on covariates that are also related to the longitudinal and time-to-event processes (see Tables 2 and 3). Model 2, which uses the same covariates as those considered in the class-specific JM, provides consistently satisfactory performance regardless of the ground truth, offering much better estimation accuracy in Scenarios 3 and 4 (see Tables 2 and 3) and similar accuracy in Scenarios 1 and 2 (see Supplemental Tables 2 and 3) compared to Model 1. Note that the classification performance appears to be minimally impacted by these specifications. Although not shown here, we conducted additional analyses under various settings. We considered an alternative version of Model 1, where

Scenario	Criteria	True number of classes (%)		
		$z = 1.65 (\alpha = 5\%)$	$z = 2.33 (\alpha = 1\%)$	$z = 3.09 (\alpha = 0.1\%)$
Scenario 1 ($G = 1$)	LOOIC	72.0	82.8	89.8
	WAIC	33.8	65.6	84.7
Scenario 2 ($G = 2$)	LOOIC	67.0	80.9	90.4
	WAIC	23.4	47.3	76.1
Scenario 3 ($G = 3$)	LOOIC	77.7	83.8	88.8
	WAIC	45.2	68.0	85.8

Table 1: Performance of LOOIC and WAIC under simulation Setting I. Model comparison and selection were performed as described in Section 3.4 of the main paper. Three different critical values for the z-score, corresponding to one-tailed tests with significance levels of 5%, 1%, and 0.1%, were considered. For each significance level, the true number of classes (%) was computed as the proportion of times the correct number of classes was selected, based on 157, 188, and 197 replications of data for Scenarios 1, 2, and 3, respectively. Not all of the 200 replications were used because, when fitting models with G larger than the true number of classes, sampling may have broken down due to class collapse, and the results from those replications were excluded.

Parameter	True Value	Model 1			Model 2		
		Bias	SD	Coverage (%)	Bias	SD	Coverage (%)
$\beta_{1,0}$	8.03	-0.002	0.142	94.0	-0.002	0.141	94.5
$\beta_{1,1}$	-0.16	0.001	0.011	94.0	0.000	0.011	95.5
$\beta_{1,2}$	-5.86	-0.100	0.143	85.5	-0.002	0.143	94.5
$\beta_{2,0}$	-8.03	0.009	0.034	94.5	0.002	0.034	94.0
$\beta_{2,1}$	0.46	-0.062	0.072	83.5	0.002	0.071	94.5
$\beta_{2,2}$	12.2	-0.141	0.082	53.0	-0.004	0.072	94.0
$\gamma_{1,0}$	-4.85	-0.336	0.473	85.5	-0.031	0.413	94.0
$\gamma_{1,1}$	-0.02	-0.002	0.007	91.0	-0.001	0.006	92.5
$\gamma_{2,0}$	-4.85	-0.172	0.276	87.5	-0.026	0.283	94.0
$\gamma_{2,1}$	0.09	0.002	0.005	92.5	0.000	0.005	94.0
α_1	0.38	0.021	0.037	90.5	0.001	0.034	93.5
α_2	0.08	-0.008	0.010	82.0	0.000	0.009	94.5
ξ_1	1.8	0.121	0.129	85.5	0.023	0.117	97.5
ξ_2	1.4	0.006	0.058	93.5	0.011	0.058	93.5
σ_1^2	0.4761	0.000	0.015	94.0	0.001	0.015	94.0
σ_2^2	0.4761	-0.005	0.023	96.0	-0.007	0.023	96.0
$\Sigma_{1,11}$	0.87	-0.083	0.066	80.0	-0.001	0.072	94.5
$\Sigma_{1,22}$	0.02	0.000	0.002	95.5	0.001	0.002	96.0
$\Sigma_{2,11}$	0.02	0.031	0.025	74.5	0.015	0.019	92.5
$\Sigma_{2,22}$	0.91	-0.016	0.096	93.5	-0.004	0.098	95.0
		Classification accuracy			Classification accuracy		
		97.4 (97.0, 97.9)			99.1 (98.9, 99.3)		

Table 2: Results for simulation Setting II (Scenario 3). For each parameter, bias and standard deviation (SD) are evaluated based on the posterior mean obtained from 200 data replications, and coverage is the proportion of times the 95% credible interval contains the true parameter value across the 200 replications. Classification accuracy is summarized using the median and interquartile range (shown in brackets), with accuracy for each replication calculated as the proportion of correctly classified subjects. Model 1: model with homogeneous mixture weights (ignoring covariate effects on the class membership). Model 2: model with covariate dependent mixture weights (use gender and age only).

Parameter	True Value	Model 1			Model 2		
		Bias	SD	Coverage (%)	Bias	SD	Coverage (%)
$\beta_{1,0}$	8.03	-0.023	0.127	94.5	-0.025	0.127	96.0
$\beta_{1,1}$	-0.16	0.001	0.010	95.5	0.000	0.010	95.5
$\beta_{1,2}$	-5.86	-0.071	0.144	87.5	0.026	0.144	93.5
$\beta_{2,0}$	-8.03	0.011	0.033	93.5	0.004	0.032	93.5
$\beta_{2,1}$	0.46	-0.061	0.076	81.5	0.000	0.079	89.0
$\beta_{2,2}$	12.2	-0.134	0.083	53.5	-0.011	0.072	96.5
$\gamma_{1,0}$	-4.85	-0.370	0.435	86.5	-0.062	0.397	93.0
$\gamma_{1,1}$	-0.02	-0.001	0.006	95.0	-0.001	0.006	96.0
$\gamma_{2,0}$	-4.85	-0.176	0.261	91.5	-0.051	0.267	95.0
$\gamma_{2,1}$	0.09	0.002	0.004	93.5	0.001	0.005	94.5
α_1	0.38	0.025	0.034	88.5	0.004	0.032	96.0
α_2	0.08	-0.007	0.009	86.0	0.000	0.009	97.5
ξ_1	1.8	0.128	0.132	82.0	0.031	0.123	95.5
ξ_2	1.4	0.005	0.051	94.0	0.010	0.052	94.0
σ_1^2	0.4761	0.000	0.014	93.5	0.001	0.014	94.5
σ_2^2	0.4761	-0.004	0.026	95.0	-0.006	0.025	94.0
$\Sigma_{1,11}$	0.87	-0.064	0.071	84.5	0.012	0.076	94.5
$\Sigma_{1,22}$	0.02	0.000	0.002	93.5	0.001	0.002	94.5
$\Sigma_{2,11}$	0.02	0.034	0.026	73.0	0.018	0.019	88.5
$\Sigma_{2,22}$	0.91	-0.009	0.086	97.5	0.002	0.087	98.0
		Classification accuracy			Classification accuracy		
		97.5 (97.1, 98.0)			99.0 (98.8, 99.3)		

Table 3: Results for simulation Setting II (Scenario 4). The settings are the same as those in Table 2.

the softmax parametrisation for the class membership submodel is replaced by a Dirichlet model on the homogeneous mixture weights, with the concentration parameter set to 1. The results are nearly identical, and the key patterns remaining unchanged. When G is not fixed, we found that ignoring relevant covariates in the membership submodel also impacts the selection of the number of classes. In particular, we found that this omission can be compensated for by selecting additional classes. Clearly, the extent of the bias incurred and the impact on inference depend on the strength of the association between the covariates and the class allocation and longitudinal processes. In general, we would expect the impact to increase as the strength of the association grows.

5 Application to the PAQUID dataset

We illustrate our proposed method using the PAQUID dataset available from the `1cmm` R package, which consists of a random subsample of 500 subjects from the prospective cohort study of the same name, aimed at investigating the relationship between risk factors and cognitive and functional aging diseases in the elderly population in France. The study participants were aged 65 and over at entry and were drawn from two regions in southwestern France. Information on baseline socio-demographic variables, cognitive performance, and health and medical history were recorded at an individual level over a maximum follow up period of 20 years. For more background information on the original data, we refer to Proust-Lima et al. (2017) and the references therein. Proust-Lima et al. (2017) used the basic JLCM to examine the trajectory of repeated

measures of a normalized version of the Mini-Mental State Examination score (normMMSE) with age and the associated risk of dementia. For this analysis, 1 subject was removed due to the event of interest occurring earlier than the entry time ($n = 499$). The number of longitudinal measurements per individual had a median of 4 and an interquartile range of (2, 7), and 74.3% of subjects had censored event times. Using the basic JLCM, model selection on the number of latent classes was performed based on the BIC, and $G = 4$ latent classes was suggested. Interestingly, with $G = 4$, the hypothesis testing performed therein indicated that the conditional independence of the longitudinal and time-to-event outcomes, given latent class, was not supported by the data.

Here, motivated by the analysis conducted in Proust-Lima et al. (2017), we use the shared parameter JLCM to re-analyse the same data to explore any changes in the latent class structure and to investigate the relationship between normMMSE and the risk of dementia within a latent class, which remains unexplored in earlier works. The basic setup for the longitudinal and time-to-event submodels mostly follows the JLCM used in Proust-Lima et al. (2017). To simplify prior specification and improve sampling efficiency, we further standardised the normMMSE (which ranges from 0 to 100) to have a mean of 0 and a standard deviation of 1. The longitudinal trajectory for the standardized normMMSE, conditional on the class membership k , is modelled via a LMM as

$$(y_{ij} | c_i = g) = \beta_{g0} + \beta_{g1}age65_{ij} + \beta_{g2}age65_{ij}^2 + b_{ig0} + b_{ig1}age65_{ij} + b_{ig2}age65_{ij}^2 + \beta_{g,CEP}CEP_i + \epsilon_{igj}, \quad (16)$$

where $age65_{ij} = (age_{ij} - 65)/10$, with age_{ij} being the age of individual i at the j th visit, and CEP_i is a binary variable for education, where 1 indicates the subject graduated with a primary school diploma, and 0 otherwise. We further assumed that $(b_{ig0}, b_{ig1}, b_{ig2}) \sim N(0, \Sigma_g)$, with Σ_g being diagonal, and that $\epsilon_{igj} \sim N(0, \sigma_g^2)$. For the class-specific time-to-event submodel, we used the same time scale (i.e., $age65_{ij}$) as for the longitudinal process, and we link the time-to-event process with the longitudinal process using a current value association. The hazard function is specified as

$$h_i(t | c_i = g) = h_{0g}(t) \exp(\gamma_{g,CEP}CEP_i + \gamma_{g,male}male_i + \gamma_{g,CEP \times male}(CEP_i \times male_i) + \alpha_g \mu_{ig}(t)), \quad (17)$$

where $h_{0g}(t) = \phi_{g0}t^{\phi_{g0}-1} \exp(\phi_{g1})$, $male_i$ is a binary variable, with 1 for male and 0 for female, and $\mu_{ig}(t)$ is the conditional mean of $y_i(t)$ given $c_i = g$. The interaction term was not considered in the previous JLCM, but we include it here to assess whether an interaction effect between gender and education occurs. We also note that Proust-Lima et al. (2017) did not incorporate covariates into the class membership submodel. In our analysis, however, motivated by our findings from the simulation study, we chose to include both CEP_i and $male_i$ to guard against the possibility of incurring any bias on the estimation results. The membership submodel is therefore specified as

$$\pi_{ig} = P(c_i = g) = \frac{\exp(\psi_{g0} + \psi_{g,CEP}CEP_i + \psi_{g,male}male_i)}{\sum_{k=1}^G \exp(\psi_{k0} + \psi_{k,CEP}CEP_i + \psi_{k,male}male_i)}, \quad g = 1, \dots, G, \quad (18)$$

where ψ_{G0} , $\psi_{G,CEP}$ and $\psi_{G,male}$ are set to zeros. To complete the Bayesian model, we choose the following

set of prior distributions:

$$\begin{aligned} \beta_{g\cdot}, \psi_{g\cdot} &\sim N(0, 2^2), & \gamma_{g\cdot}, \phi_{g1}, \alpha_g &\sim N(0, 3^2), & \phi_{g0} &\sim \text{Gamma}(2, 0.5), \\ \sigma_g^2 &\sim \text{half-Normal}(0, 0.2^2), & \Sigma_{g,ii} &\sim \text{Gamma}(1.5, 1.5). \end{aligned} \tag{19}$$

Note that we used generally more informative normal priors for the fixed effect parameters than in the simulation study, partly due to the smaller sample size here, and we also accounted for the fact that the longitudinal data had been standardized. The hyperparameters for the priors on the variance parameters were informed by the MLE results obtained from the `lcm` R package, as was done in the simulation study.

We first examine the number of latent classes using the approach described in Section 3.4, considering candidate values of G ranging from one to four due to the relatively small sample size. Posterior inference was based on $M = 6$ parallel chains, each run for 12000 iterations (for $G = 1, 2, 3$) or 14000 iterations (for $G = 4$), with the first 4000 (for $G = 1, 2, 3$) or 6000 (for $G = 4$) iterations discarded as burn-in, based on pilot runs and convergence diagnostics. For each chain, the 8000 post burn-in samples were further thinned by an interval of 4. The other estimation settings are the same as in the simulation study. Table 4 shows the results of the estimated LOOIC and WAIC for different values of G (on the deviance scale), as well as the associated z-score for testing the difference in LOOIC or WAIC between models with $G = k$ and $G = k + 1$. The largest drop in both LOOIC and WAIC occurs when increasing G from one to two, with the z-scores associated with the difference in LOOIC and WAIC both greater than 5.6 (and p-values effectively zero), indicating strong support for the presence of a latent class structure. $G = 4$ achieves the smallest LOOIC and WAIC; however, the improvement it offers over $G = 3$ is minimal, as indicated by the associated z-scores (and p-values) for LOOIC and WAIC. Additionally, when examining the estimated latent class structure with $G = 4$, an extra small cluster is generated with only three individuals assigned to it. Therefore, we may be skeptical in considering this as a meaningful ‘subgroup’. Comparing models with two and three latent classes, there seems to be moderate evidence for the difference in LOOIC and WAIC, as indicated by the associated z-scores and p-values. Figure 1 displays the class-specific longitudinal trajectories and Kaplan-Meier survival curves based on the estimated models with $G = 2$ (top panel) and $G = 3$ (bottom panel). Class membership for each individual was assigned based on the maximum posterior class probability, as done in the simulation study. It appears that class 2 in the model with $G = 2$, which is associated with more significant declines in normMMSE and a more rapid progression of dementia, is further split into two subclasses in the model with $G = 3$ (labelled as subgroups 1 and 3). This visual impression is confirmed by comparing the class allocation results obtained from $G = 2$ and $G = 3$. Depending on the desired level of detail, either model could be of interest. Here, we focus on $G = 2$ to capture the major subgroup structures within the study cohort. Based on the estimated class allocation, 75.8% (377/499) of individuals are classified into class 1, the relatively lower-risk group, while the remaining belong to class 2. Table 5 shows the posterior means and 95% credible intervals for key parameters of interest in the model with $G = 2$. The male gender shows a significant association with class membership ($\psi_{1,male}$), where, prior to observing any longitudinal data, being male increases the chance of being classified into the relatively lower-risk group.

Additionally, there is a strong association between normMMSE and dementia, conditional on latent class membership, as indicated by the magnitude of α_k and the fact that the associated credible intervals exclude zero. The strength of the association is similar across both subgroups. The negative relationship is expected, as higher normMMSE generally reflects better cognitive function, which is anticipated to be associated with a lower risk of cognitive diseases such as dementia. The log-hazard ratio for education, $\gamma_{g,CEP}$, is estimated to be positive. While this may seem contradictory to earlier results in Proust-Lima et al. (2017) where CEP had a protective effect on dementia, it is important to note that here the effect of CEP is mediated through the longitudinal marker (MMSE) via $\mu_i(t)$. The total effect of CEP on the risk of dementia, given by $\gamma_{g,CEP} + \alpha_g \times \beta_{g,CEP} + \gamma_{g,CEP \times male} \times male_i$, remains negative. Another observation is that the two subgroups exhibit different levels of within-group variability in normMMSE (measured via σ_g^2), with the higher-risk group, class 2, showing greater within-class variability. This aligns with the clinical literature, which links neurodegenerative disorders to increased intraindividual variability in cognitive performance metrics (Hultsch et al. 2000, Gorus et al. 2008).

	LOOIC	Z_{LOOIC}	P_{LOOIC}	WAIC	Z_{WAIC}	P_{WAIC}
G = 1	4299	5.62	0	4068	6.97	0
G = 2	4118	2.82	0.002	3850	2.66	0.004
G = 3	4063	1.07	0.142	3802	0.63	0.264
G = 4	4033	-	-	3781	-	-

Table 4: Results for comparing models with candidate values of G . For each $G = k$, LOOIC and WAIC (on the deviance scale) are computed as described in Sections 3.4 and 5. The Z_{LOOIC} and Z_{WAIC} represent the z-scores associated with the differences in LOOIC and WAIC, respectively, comparing models with $G = k$ and $G = k+1$. P_{LOOIC} and P_{WAIC} are the one-tailed p-values associated with Z_{LOOIC} and Z_{WAIC} , respectively.

	Parameters	Estimates (Posterior Mean (95% CI))	
		Class 1	Class 2
Longitudinal submodel	$\beta_{g,CEP}$	0.851 (0.670, 1.040)	0.365 (-0.013, 0.705)
	σ_g^2	0.223 (0.191, 0.252)	0.316 (0.268, 0.370)
Time-to-event submodel	α_g	-3.697 (-5.308, -2.388)	-3.602 (-4.862, -2.581)
	$\gamma_{g,CEP}$	1.155 (-0.078, 2.466)	0.460 (-0.506, 1.334)
	$\gamma_{g,male}$	0.424 (-1.053, 1.890)	0.144 (-1.581, 1.666)
	$\gamma_{g,CEP \times male}$	0.921 (-1.029, 2.949)	-0.016 (-1.810, 1.943)
Membership submodel	ψ_{10}	0.502 (-0.244, 1.315)	
	$\psi_{1,CEP}$	-0.245 (-1.016, 0.507)	
	$\psi_{1,male}$	0.904 (0.214, 1.581)	

Table 5: Estimation results for the shared parameter JLCM with $G = 2$.

6 Discussion

In this paper, we focus on shared parameter JLCMs, which provide an important extension of the standard JM for study populations of a heterogeneous nature. We propose a new Bayesian inferential framework to effectively tackle the computational challenges faced by existing Bayesian methods. To enhance sampling

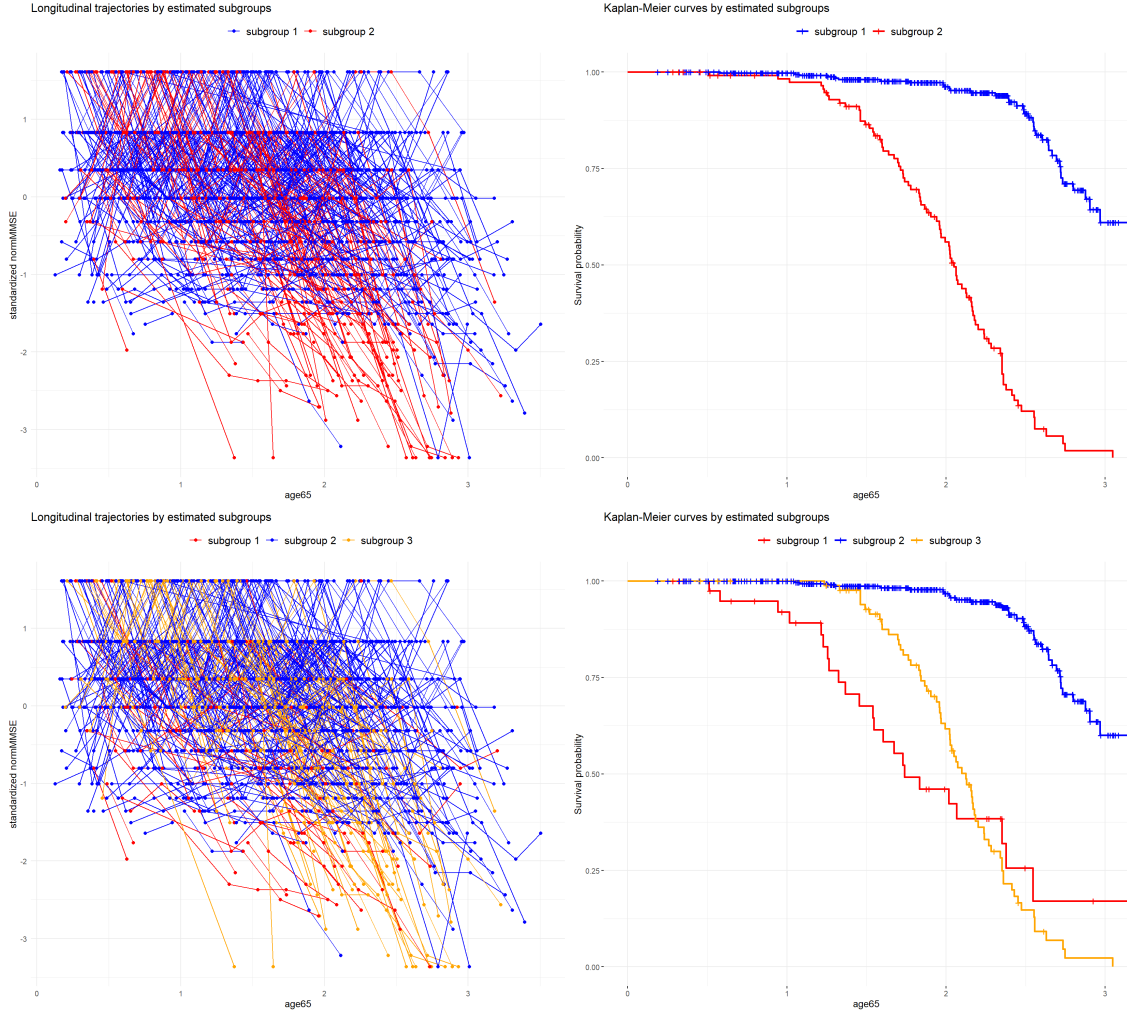


Figure 1: Trajectories of standardized normMMSE and Kaplan-Meier curves by estimated subgroups (indicated by colours). The top panel displays results for $G = 2$, and the bottom panel for $G = 3$.

efficiency, we adopt a strategy that enables the use of state-of-the-art MCMC methods. We effectively address potential multimodality in the posterior through a parallel sampling scheme, leveraging parallel computing power. Model selection for the number of latent classes can be guided by predictive-based criteria such as LOOIC, which are conveniently estimated from MCMC output. Through a simulation study, we demonstrate that the proposed method provides superior estimation accuracy compared to the existing approach. The feasibility of our method is further illustrated via an application to the PAQUID data, where we explored the underlying latent class structure and obtained insights into the association between the cognitive measure MMSE and the risk of dementia within each latent class.

Our results bring important insights to the practical implementation of such models. One important aspect regards the prior specification, which has received very little discussion in the context of shared parameter JLCMs. Unlike the standard JM, prior specifications for JLCMs require additional care. It is desirable to use relatively informative priors that exploit available knowledge, perhaps in conjunction with empirical Bayes strategies, which can help with model identifiability and the convergence of the algorithm. Sensitivity analysis may be performed to examine the impact in specific application contexts. Regarding

selection on the number of latent classes, our results suggest that predictive-based criteria such as LOOIC can be informative, though the hypothesis testing procedure introduced in Section 3.4 (i.e., testing whether the improvement offered by the more complex model is truly significant) is necessary to guard against the risk of overfitting. In particular, a more conservative approach (i.e., using a relatively stringent significance level) seems necessary. We also found that including relevant covariates in the class membership model is important. While ignoring these covariates has minimal impact on classification accuracy, bias arises when they are related to the longitudinal and time-to-event processes. Therefore, it seems advisable to include the same set of covariates considered in class-specific JMs to mitigate potential bias.

From the modelling perspective, it is possible to extend the algorithm considered here to alternative formulations of JLCMs, depending on the application context. For instance, when the focus is on prediction and multivariate longitudinal markers are present, we could replace the shared parameter structure with a two-stage approach, where summaries from the raw longitudinal data are first extracted and treated as time-varying covariates in the time-to-event submodel (Alvares & Leiva-Yamaguchi 2023). A specific formulation under a discrete hazard framework using a frequentist approach has been considered in Nguyen et al. (2023). A Bayesian formulation under a more generic hazard setting may provide advantages in terms of prior regularization, prediction, and associated uncertainty quantification. From the algorithmic perspective, it would be interesting to explore alternative approximate Bayesian inference methods that are potentially more scalable in complex, large-data settings. The MCMC-based method presented here can serve as a gold standard benchmark for evaluating these approximate algorithms. One option, motivated by the recent success of INLA for the standard JMs (Rustand et al. 2024, Alvares et al. 2024), is the possibility of adapting it to the mixture setting by combining MCMC with INLA (Gómez-Rubio & Rue 2018). In this approach, we sample from the marginal posterior of the latent class allocation variables using MCMC, and conditional on the sampled class allocation, INLA is used to fit the class-specific JM. Some preliminary experiments (not reported here) suggest that the efficiency was extremely low due to the poor acceptance rate of the MCMC step and stability issues with INLA, which arise from the need to refit the model a large number of times. A more efficient MCMC proposal and a more stable or dedicated version of the INLA program warrant further development. Variational-based methods could offer another promising option. Black-box variational algorithms, such as those provided by Stan, are not feasible for such complex models. A customized development, possibly building on recent advances in variational inference algorithms for standard JMs (Sun & Basu 2024), would be of interest.

Acknowledgements

SC and MP were supported by the UK Medical Research Council (MRC) grant “Looking beyond the mean: what within-person variability can tell us about dementia, cardiovascular disease and cystic fibrosis” (MR/V020595/1). DA and JKB were supported by MRC Unit Programme MC_UU_00002/5.

References

- Alvares, D. & Leiva-Yamaguchi, V. (2023), ‘A two-stage approach for Bayesian joint models: Reducing complexity while maintaining accuracy’, *Statistics and Computing* **33**(5), 1–11.
- Alvares, D., Van Niekerk, J., Krainski, E. T., Rue, H. & Rustand, D. (2024), ‘Bayesian survival analysis with INLA’, *Statistics in Medicine* **43**(20), 3975–4010.
- Andrinopoulou, E. R., Nasserinejad, K., Szczesniak, R. & Rizopoulos, D. (2020), ‘Integrating latent classes in the Bayesian shared parameter joint model of longitudinal and survival outcomes’, *Statistical Methods in Medical Research* **29**(11), 3294–3307.
- Barrett, J. K., Huille, R., Parker, R., Yano, Y. & Griswold, M. (2019), ‘Estimating the association between blood pressure variability and cardiovascular disease: An application using the ARIC study’, *Statistics in Medicine* **38**(10), 1855–1868.
- Chen, S. & Finkenstädt, B. (2023), ‘Bayesian spline-based hidden Markov models with applications to actimetry data and sleep analysis’, *Journal of the American Statistical Association* pp. 1–11.
- Gómez-Rubio, V. & Rue, H. (2018), ‘Markov chain Monte Carlo with the integrated nested Laplace approximation’, *Statistics and Computing* **28**, 1033–1051.
- Gorus, E., De Raedt, R., Lambert, M., Lemper, J.-C. & Mets, T. (2008), ‘Reaction times and performance variability in normal aging, mild cognitive impairment, and Alzheimer’s disease’, *Journal of Geriatric Psychiatry and Neurology* **21**(3), 204–218.
- Hoffman, M. D., Gelman, A. et al. (2014), ‘The No-U-Turn sampler: Adaptively setting path lengths in Hamiltonian Monte Carlo’, *Journal of Machine Learning Research* **15**(1), 1593–1623.
- Hultsch, D. F., MacDonald, S. W., Hunter, M. A., Levy-Bencheton, J. & Strauss, E. (2000), ‘Intraindividual variability in cognitive performance in older adults: Comparison of adults with mild dementia, adults with arthritis, and healthy adults’, *Neuropsychology* **14**(4), 588.
- Letenneur, L., Commenges, D., Dartigues, J.-F. & Barberger-Gateau, P. (1994), ‘Incidence of dementia and Alzheimer’s disease in elderly community residents of south-western France’, *International Journal of Epidemiology* **23**(6), 1256–1261.
- Liu, Y., Lin, Y., Zhou, J. & Liu, L. (2020), ‘A semi-parametric joint latent class model with longitudinal and survival data’, *Statistics and Its Interface* **13**(3), 411–422.
- Liu, Y., Liu, L. & Zhou, J. (2015), ‘Joint latent class model of survival and longitudinal data: An application to CPCRA study’, *Computational Statistics & Data Analysis* **91**, 40–50.
- Llorente, F., Martino, L., Delgado, D. & Lopez-Santiago, J. (2023), ‘Marginal likelihood computation for model selection and hypothesis testing: An extensive review’, *SIAM review* **65**(1), 3–58.

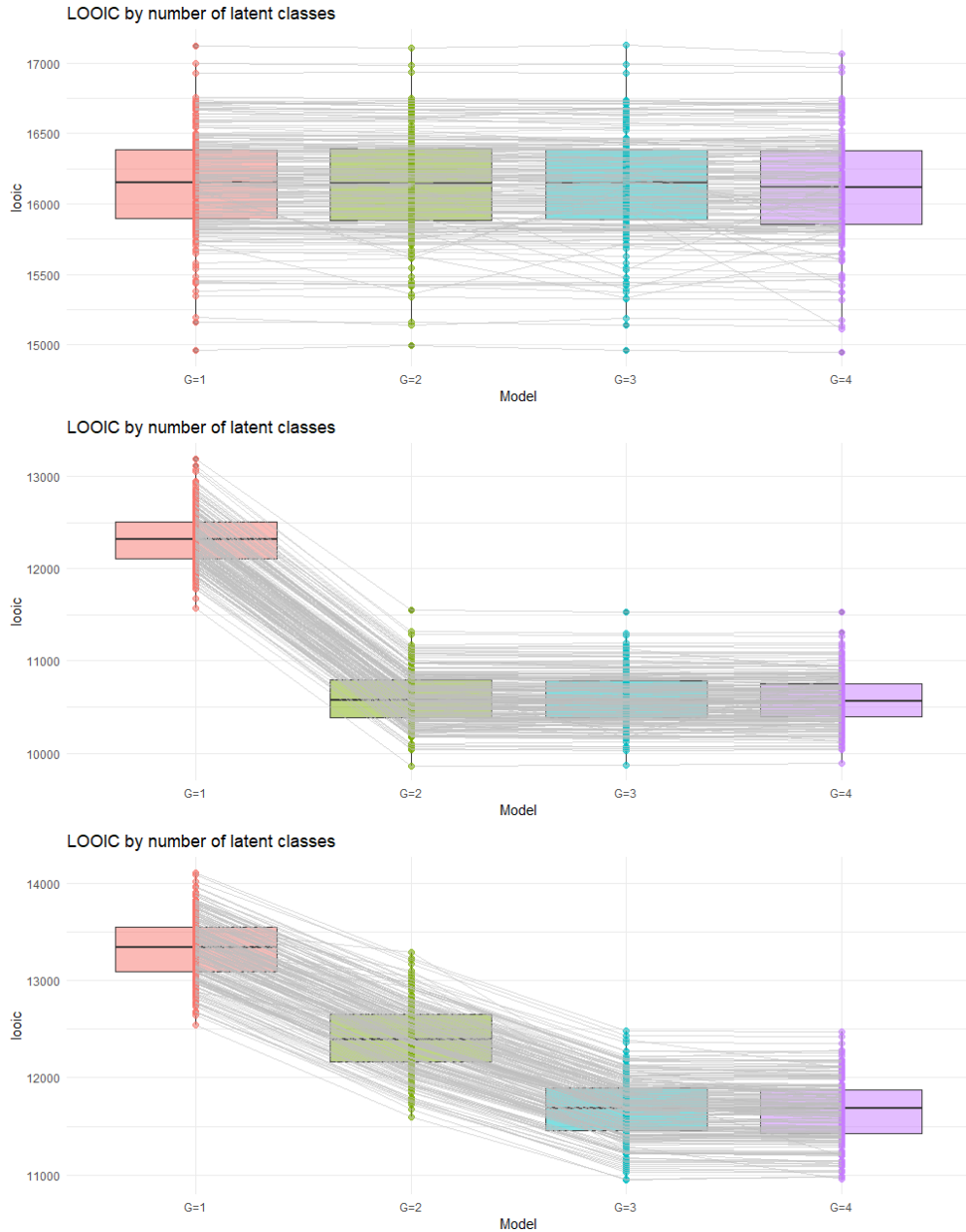
- Nguyen, V. T., Fermanian, A., Guilloux, A., Barbieri, A., Zohar, S., Jannot, A.-S. & Bussy, S. (2023), ‘FLASH: A fast joint model for longitudinal and survival data in high dimension’, *arXiv preprint arXiv:2309.03714* .
- Papageorgiou, G., Mauff, K., Tomer, A. & Rizopoulos, D. (2019), ‘An overview of joint modeling of time-to-event and longitudinal outcomes’, *Annual Review of Statistics and Its Application* **6**(1), 223–240.
- Proust-Lima, C., Philipps, V., Diakite, A. & Liqueet, B. (2023), *lcmm: Extended Mixed Models Using Latent Classes and Latent Processes*. R package version: 2.1.0.
URL: <https://cran.r-project.org/package=lcmm>
- Proust-Lima, C., Philipps, V. & Liqueet, B. (2017), ‘Estimation of extended mixed models using latent classes and latent processes: The R package lcmm’, *Journal of Statistical Software* **78**(2), 1–56.
- Proust-Lima, C., Séne, M., Taylor, J. M. & Jacqmin-Gadda, H. (2014), ‘Joint latent class models for longitudinal and time-to-event data: A review’, *Statistical Methods in Medical Research* **23**(1), 74–90.
- Rizopoulos, D. (2012), *Joint models for longitudinal and time-to-event data: With applications in R*, Chapman & Hall/CRC.
- Robert, C. P. & Wraith, D. (2009), ‘Computational methods for Bayesian model choice’, *AIP Conference Proceedings* **1193**(1), 251–262.
- Rustand, D., Van Niekerk, J., Krainski, E. T., Rue, H. & Proust-Lima, C. (2024), ‘Fast and flexible inference for joint models of multivariate longitudinal and survival data using integrated nested Laplace approximations’, *Biostatistics* **25**(2), 429–448.
- Sivula, T., Magnusson, M., Matamoros, A. A. & Vehtari, A. (2020), ‘Uncertainty in Bayesian leave-one-out cross-validation based model comparison’, *arXiv preprint arXiv:2008.10296* .
- Smith, A. F. & Gelfand, A. E. (1992), ‘Bayesian statistics without tears: A sampling–resampling perspective’, *The American Statistician* **46**(2), 84–88.
- Stan Development Team (2024), ‘RStan: The R interface to Stan’. R package version 2.32.6.
URL: <https://mc-stan.org/>
- Stephens, M. (2000), ‘Dealing with label switching in mixture models’, *Journal of the Royal Statistical Society: Series B (Statistical Methodology)* **62**(4), 795–809.
- Štrumbelj, E., Boucharde-Côté, A., Corander, J., Gelman, A., Rue, H., Murray, L., Pesonen, H., Plummer, M. & Vehtari, A. (2024), ‘Past, present and future of software for Bayesian inference’, *Statistical Science* **39**(1), 46–61.
- Su, W., Wang, X. & Szczesniak, R. D. (2021), ‘Risk factor identification in cystic fibrosis by flexible hierarchical joint models’, *Statistical Methods in Medical Research* **30**(1), 244–260.

- Sun, J. & Basu, S. (2024), ‘Penalized joint models of high-dimensional longitudinal biomarkers and a survival outcome’, *The Annals of Applied Statistics* **18**(2), 1490–1505.
- Vehtari, A., Gabry, J., Magnusson, M., Yao, Y., Bürkner, P.-C., Paananen, T. & Gelman, A. (2024), ‘loo: Efficient leave-one-out cross-validation and WAIC for Bayesian models’. R package version 2.8.0.
URL: <https://mc-stan.org/loo/>
- Vehtari, A., Gelman, A. & Gabry, J. (2017), ‘Practical Bayesian model evaluation using leave-one-out cross-validation and WAIC’, *Statistics and Computing* **27**, 1413–1432.
- Vehtari, A., Gelman, A., Simpson, D., Carpenter, B. & Bürkner, P.-C. (2021), ‘Rank-normalization, folding, and localization: An improved \hat{R} for assessing convergence of MCMC (with discussion)’, *Bayesian Analysis* **16**(2), 667–718.
- Wong, K. Y., Zeng, D. & Lin, D. (2022), ‘Semiparametric latent-class models for multivariate longitudinal and survival data’, *Annals of Statistics* **50**(1), 487.
- Yao, Y., Vehtari, A. & Gelman, A. (2022), ‘Stacking for non-mixing Bayesian computations: The curse and blessing of multimodal posteriors’, *Journal of Machine Learning Research* **23**(79), 1–45.

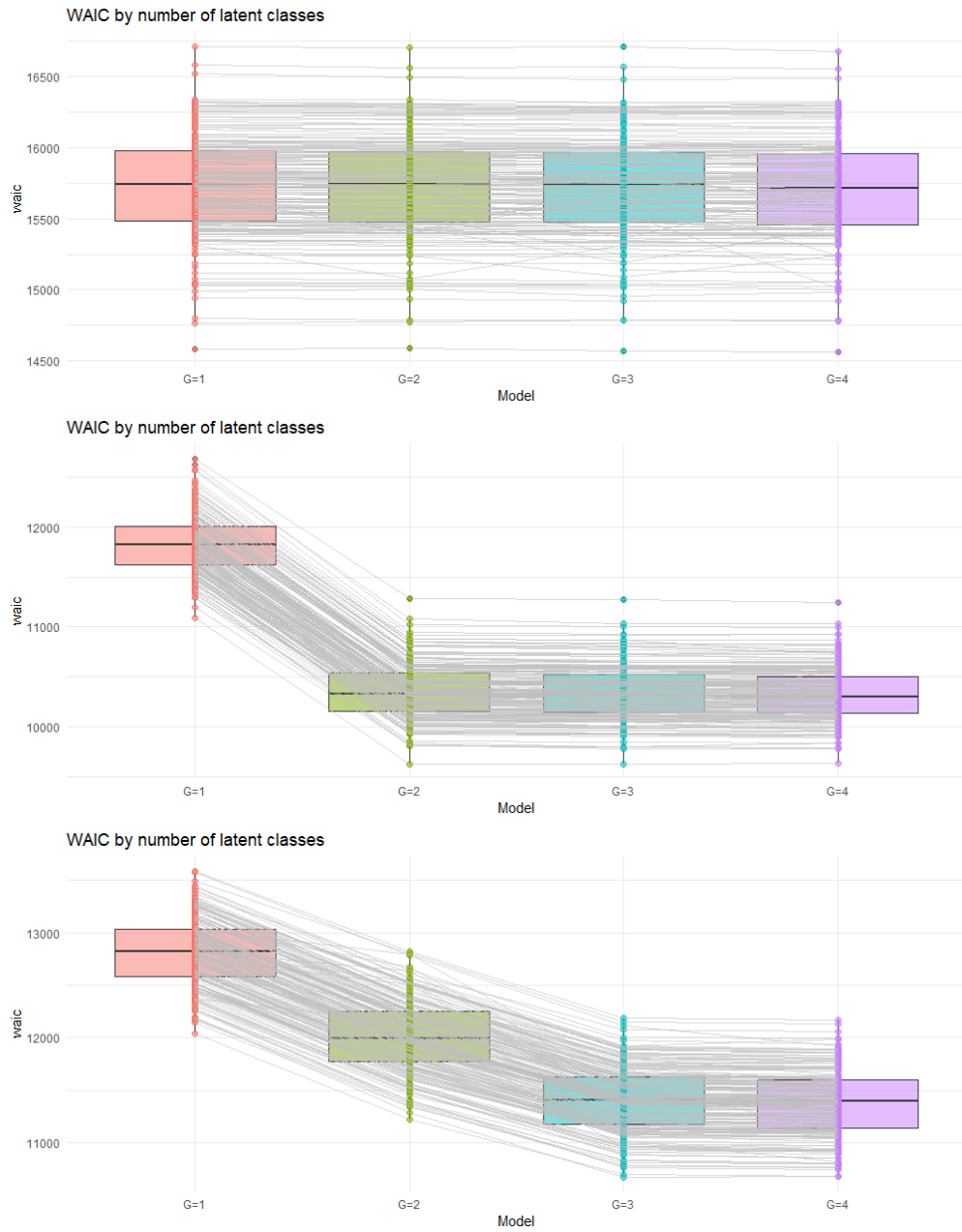
Supplementary material to the paper Bayesian shared parameter joint models for heterogeneous populations

Sida Chen, Danilo Alvares, Marco Palma, Jessica K. Barrett

MRC Biostatistics Unit, University of Cambridge, U.K.



Supplementary Figure 1: Boxplot summary of LOOIC (on the deviance scale) computed for candidate values of G based on 200 data replications for Scenario 1 (top panel), Scenario 2 (middle panel), and Scenario 3 (bottom panel) from simulation Setting I. Points representing LOOIC for specific data replications are superimposed on the boxplots and are connected by lines when based on the same data replication.



Supplementary Figure 2: Boxplot summary of WAIC (on the deviance scale) computed for candidate values of G based on 200 data replications for Scenario 1 (top panel), Scenario 2 (middle panel), and Scenario 3 (bottom panel) from simulation Setting I. Points representing WAIC for specific data replications are superimposed on the boxplots and are connected by lines when based on the same data replication.

Parameter	True Value	Bias	SD	Coverage (%)
$\beta_{1,0}$	8.03	0.009	0.143	95.5
$\beta_{1,1}$	-0.16	0.000	0.023	95.5
$\beta_{1,2}$	-5.86	-0.009	0.207	96.5
$\beta_{2,0}$	-8.03	-0.004	0.051	93.0
$\beta_{2,1}$	0.46	0.009	0.094	94.0
$\beta_{2,2}$	12.2	-0.003	0.072	93.0
$\beta_{3,0}$	0.03	0.001	0.046	96.5
$\beta_{3,1}$	-0.01	-0.002	0.035	93.5
$\beta_{3,2}$	-1.96	0.001	0.061	97.0
$\gamma_{1,0}$	-4.85	-0.165	0.807	93.5
$\gamma_{1,1}$	-0.02	-0.002	0.011	95.0
$\gamma_{2,0}$	-4.85	-0.079	0.300	96.0
$\gamma_{2,1}$	0.09	0.001	0.006	96.5
$\gamma_{3,0}$	2.85	0.036	0.228	94.5
$\gamma_{3,1}$	-0.12	-0.002	0.007	93.5
α_1	0.38	0.014	0.066	93.5
α_2	0.08	0.002	0.011	92.0
α_3	0.58	0.010	0.034	96.5
ξ_1	1.8	0.065	0.228	95.0
ξ_2	1.4	0.020	0.066	95.5
ξ_3	1.8	0.032	0.088	91.5
σ_1^2	0.4761	0.002	0.030	95.0
σ_2^2	0.4761	-0.006	0.029	94.0
σ_3^2	0.4761	-0.001	0.015	95.5
$\Sigma_{1,11}$	0.87	0.025	0.166	93.5
$\Sigma_{1,22}$	0.02	0.003	0.007	94.0
$\Sigma_{2,11}$	0.02	0.021	0.020	92.5
$\Sigma_{2,22}$	0.91	0.013	0.118	97.0
$\Sigma_{3,11}$	0.28	0.006	0.035	94.0
$\Sigma_{3,22}$	0.31	0.002	0.028	95.0

Supplementary Table 1: Results for simulation Setting I (Scenario 3) with G fixed at 3. For each parameter, bias and standard deviation (SD) are evaluated based on the posterior mean obtained from 200 data replications, and coverage is the proportion of times the 95% credible interval contains the true parameter value across the 200 replications.

Parameter	True Value	Model 1			Model 2		
		Bias	SD	Coverage (%)	Bias	SD	Coverage (%)
$\beta_{1,0}$	8.03	-0.006	0.085	93.5	-0.006	0.084	94.0
$\beta_{1,1}$	-0.16	0.000	0.014	94.0	0.000	0.014	95.0
$\beta_{1,2}$	-5.86	0.018	0.127	94.5	0.019	0.124	96.0
$\beta_{2,0}$	-8.03	0.001	0.032	95.0	0.001	0.033	94.5
$\beta_{2,1}$	0.46	-0.006	0.063	93.5	-0.006	0.063	94.5
$\beta_{2,2}$	12.2	-0.005	0.048	93.5	-0.005	0.049	93.0
$\gamma_{1,0}$	-4.85	-0.024	0.428	94.5	-0.023	0.433	93.5
$\gamma_{1,1}$	-0.02	-0.001	0.005	95.5	-0.001	0.005	96.0
$\gamma_{2,0}$	-4.85	-0.012	0.201	97.5	-0.010	0.201	96.5
$\gamma_{2,1}$	0.09	0.000	0.004	98.0	0.000	0.004	97.0
α_1	0.38	0.004	0.037	94.0	0.004	0.036	93.0
α_2	0.08	0.000	0.007	95.5	0.000	0.007	95.5
ξ_1	1.8	0.029	0.124	92.5	0.028	0.124	92.5
ξ_2	1.4	0.005	0.046	95.5	0.005	0.047	94.0
σ_1^2	0.4761	-0.001	0.019	94.0	-0.001	0.019	95.0
σ_2^2	0.4761	-0.009	0.021	91.0	-0.008	0.021	91.5
$\Sigma_{1,11}$	0.87	0.006	0.095	92.5	0.006	0.095	94.0
$\Sigma_{1,22}$	0.02	0.001	0.004	92.0	0.001	0.005	93.0
$\Sigma_{2,11}$	0.02	0.013	0.017	91.0	0.012	0.017	91.0
$\Sigma_{2,22}$	0.91	0.006	0.083	98.0	0.007	0.084	97.5
		Classification accuracy			Classification accuracy		
		98.8 (98.6, 99.0)			98.8 (98.4, 99.0)		

Supplementary Table 2: Results for simulation Setting II (Scenario 1). For each parameter, bias and standard deviation (SD) are evaluated based on the posterior mean obtained from 200 data replications, and coverage is the proportion of times the 95% credible interval contains the true parameter value across the 200 replications. Classification accuracy is summarized using the median and interquartile range (shown in brackets), with accuracy for each replication calculated as the proportion of correctly classified subjects. Model 1: model with homogeneous mixture weights (ignoring covariate effects on the class membership). Model 2: model with covariate dependent mixture weights (use gender and age only).

Parameter	True Value	Model 1			Model 2		
		Bias	SD	Coverage (%)	Bias	SD	Coverage (%)
$\beta_{1,0}$	8.03	-0.005	0.085	93.0	-0.006	0.085	92.0
$\beta_{1,1}$	-0.16	0.001	0.012	95.0	0.001	0.012	96.0
$\beta_{1,2}$	-5.86	0.004	0.121	92.5	0.005	0.121	94.0
$\beta_{2,0}$	-8.03	0.005	0.038	94.0	0.005	0.038	94.0
$\beta_{2,1}$	0.46	0.000	0.069	92.0	0.000	0.070	93.5
$\beta_{2,2}$	12.2	-0.007	0.053	96.0	-0.008	0.053	95.0
$\gamma_{1,0}$	-4.85	-0.078	0.376	94.5	-0.076	0.377	95.0
$\gamma_{1,1}$	-0.02	0.000	0.005	95.5	0.000	0.005	95.5
$\gamma_{2,0}$	-4.85	-0.036	0.243	95.0	-0.036	0.245	94.5
$\gamma_{2,1}$	0.09	0.001	0.005	95.0	0.001	0.005	94.0
α_1	0.38	0.005	0.031	95.5	0.004	0.031	95.5
α_2	0.08	0.001	0.008	95.0	0.001	0.007	96.0
ξ_1	1.8	0.030	0.111	93.5	0.029	0.112	95.5
ξ_2	1.4	0.010	0.051	94.0	0.010	0.051	94.0
σ_1^2	0.4761	0.000	0.015	95.5	0.001	0.015	97.0
σ_2^2	0.4761	-0.005	0.022	96.0	-0.005	0.022	95.5
$\Sigma_{1,11}$	0.87	0.008	0.072	96.0	0.008	0.072	97.0
$\Sigma_{1,22}$	0.02	0.001	0.003	93.5	0.001	0.003	94.0
$\Sigma_{2,11}$	0.02	0.014	0.018	87.5	0.015	0.018	91.5
$\Sigma_{2,22}$	0.91	0.017	0.085	97.0	0.015	0.085	96.0
Classification accuracy				Classification accuracy			
98.7 (98.4, 98.9)				98.7 (98.4, 98.9)			

Supplementary Table 3: Results for simulation Setting II (Scenario 2). The settings are the same as those in Table 2.